Melting of aluminum, molybdenum, and the light actinides

Marvin Ross,[1] Lin H. Yang,[1] and Reinhard Boehler[2]
[1]*Lawrence Livermore National Laboratory, Livermore, California 94551, USA*
[2]*Max-Planck-Institute fur Chemie, Postfach 3060, 6500 Mainz, Germany*
(Received 19 May 2004; published 16 November 2004)

A semiempirical model was developed in order to explain why the measured melting curves of molybdenum, and the other bcc transition metals, have an unusually low slope ($dT/dP \sim 0$). The total binding energy of Mo is written as the sum of the repulsive energy of the ions and *sp* electrons (modeled by an inverse sixth power potential) and the *d*-band cohesive energy is described by the well known Friedel equation. Using literature values for the Mo band width energy, the number of *d* electrons and their volume dependence, we find that a small broadening of the liquid *d*-band width ($\sim 1\%$) leads to an increase in the stability of the liquid relative to the solid. This is sufficient to depress the melting temperature and lower the melting slope to a value in agreement with the recent diamond-anvil cell measurements. Omission of the *d*-band physics results in an Al-like melting curve with a much steeper melt slope. The model, when applied to the *f* electrons of the light actinides (Th-Am), gives agreement with the observed fall and rise in the melting temperature with increasing atomic number.

DOI: 10.1103/PhysRevB.70.184112 PACS number(s): 61.25.Mv, 64.70.Dv

I. INTRODUCTION

Recent advances in the application of laser-heated diamond-anvil cells (DAC's) to the study of melting now enable simultaneous pressure-temperature measurements to be made in the megabar pressure range to 3000 K to 4000.[1–4] In the case of transition metals the advances have led to the discovery of unusually low melting slopes ($dT/dP \sim 0$) for the bcc metals, particularly in groups VA and VIA of the Periodic Table.[3,4] These results are at odds with conventional wisdom that melting temperatures should rise continuously with increasing pressure.[5] However, new measurements for Ta made at the Advanced Photon Source (APS),[4] using x-ray diffraction to detect melting, have confirmed the earlier results.[3] The purpose of this report is to offer a theoretical explanation as to why the transition metal melting curves have unusually low melting slopes. Mo was chosen as the test case for transition metals because it has the smallest measured melting slope of that group, and thus provides the most severe test. Subsequently, it became apparent that the same basic physics applies also to the light actinides.

In its organization, the paper first considers Al as the prototypical nearly free electron *sp* metal and is modeled here by employing the inverse-sixth power repulsive potential. The equation of state for $U_{\rm rep}$ is developed in Sec. II and applied to Al in Sec. III. In Sec. IV we consider the consequence of including *d* electrons by building on the earlier work of Ducastelle[6] and Pettifor[7] that the total binding energy of a transition metal may be written in the form $U = U_{\rm rep} + U_{d\ \rm band}$. $U_{\rm rep}$ is the repulsive contribution of the ions and *sp* electrons and $U_{d\ \rm band}$ is the cohesive energy of the *d* band. $U_{d\ \rm band}$ is included in the total energy by using the Friedel equation,[8] and the model is applied to Mo. In Sec. V the model is applied to the light actinides. The present results and their implications for melting theory are discussed in Sec. VI.

II. INVERSE-6 EQUATION OF STATE

The equations of state (EOS) for systems interacting via purely repulsive inverse power potentials

$$\phi(r) = B/r^n, \tag{1}$$

have been studied extensively by computer simulations for the hard sphere ($n=\infty$), $n=12$, 9, 6, 4 and the one component plasma ($n=1$).[9–12] An important simplifying feature of this potential is that the excess Helmholtz free energy, and all of the thermodynamic properties can be expressed as a function of a single parameter, the scaled inverse temperature

$$\Gamma_n = \beta B/(a)^n. \tag{2}$$

$\beta = 1/NkT$, a is the Wigner Seitz radius given by $4\pi n_0 a^3/3 = 1$, and n_0 is the atom number density.

The inverse sixth power is of special interest here because previous work has shown that potentials near this power best represented the *ab initio* liquid calculations of Al (Ref. 13) and Fe (Ref. 14) and served as a reference system for calculating the excess free energy needed for high pressure melting studies.

An exact analytic determination of the fcc and bcc free energies, including the first order anharmonic term, has been reported by Dubin and DeWitt[10] for the cases $n=1$ to 12. The expression for the excess solid free energy is

$$\frac{F_e^s}{NkT} = M\Gamma_n + \frac{3}{2}\ln\left\{2\left[\frac{3}{4\pi}\right]^{n/3}\Gamma_n\right\} + 1 - S_H - \frac{A_1}{\Gamma_n}. \tag{3}$$

M, S_H, and A_1 are the Madelung term, excess entropy, and first-order anharmonic constants, respectively. Values of these parameters for the inverse power potential are tabulated.[10] $M\Gamma_n$ is the Madelung energy, or the energy of the static lattice. While the terms S_H and A_1 are small, they determine the relative stability of the two solid structures near melting. The thermal internal energy, is related to the excess free energy by $U_{\rm th}/NkT = \Gamma\,\partial(F_e/NkT/\partial\Gamma)$.

The results of Monte Carlo simulations for the excess liquid energy (U_e)[8] have also been fitted[9] to analytic functions of Γ_n:

$$U_e/NkT = M\Gamma_n + U_{\rm th}/NkT. \quad (4)$$

$U_{\rm th}/NkT = b\Gamma_n^{1/4} + c$ is the thermal energy. The excess Helmholtz free energy is

$$F_e^l/NkT = M\Gamma_n + 4b\Gamma_n^{1/4} + c\ {\rm Ln}(\Gamma_n) + d. \quad (5)$$

In the case of the inverse sixth potential, $b=0.9267$ and $c=-0.584$. d is a constant of integration which must be determined for solid-liquid phase transitions.

The sixth power potential appears to be roughly the border separating the stability range of bcc and fcc phases at melting. Hoover *et al.*,[15] determined that for $n=6$, the fcc lattice is the minimum energy structure, while the looser packing of the bcc solid makes the entropy higher and favors the stability of this phase at higher temperature and near the melting. Laird and Haymet[11] have found a smaller region of bcc stability for $n=6$ than did Hoover *et al.*

More recently, Dubin and DeWitt[12] have determined that fcc, and not bcc, is the stable phase at melting for the $n=6$ and stiffer potentials. However, despite these differences there appears to be a general agreement that for values of $n \leqslant 6$, bcc is the stable crystal structure at melting and occupies an increasingly larger portion of the phase space with decreasing values of n. In the case of the one-component plasma ($n=1$), bcc is the only stable phase below the melting temperature. Dubin and DeWitt suggest that the apparent discrepancies for $n=6$ follows from the neglect of higher-order anharmonic corrections which become important near melting and allow that the fcc-bcc-liquid triple point is near $n=6$.

It is now necessary to determine a set constants in the free energy equations (3) and (5) that are in reasonable agreement with the phase diagrams predicted by L-H and D-D. Since D-D limited their calculations to the fcc-bcc phase transition, while L-H also calculated the solid-liquid transition for both structures, we used the L-H values of Γ_S and Γ_L, the solid and liquid parameters at melting and freezing respectively to adjust two of the constants.

In the case of fcc melting L-H found Γ_s and Γ_L to be 95.34 and 92.98, respectively. In order for our model to predict these values we used the liquid constants b and c cited above in Eq. (5) and set d(=2.8405) to fit the L-H excess liquid free energies. For the fcc free energy we used the parameters of D-D, $S_{H\rm fcc}=-1.6585$ and $A_{1\rm fcc}=0.416$.

To fit the L-H bcc melting parameters 94.52 and 92.17, we used the same liquid model as in fcc melting, but adjusted the value of $S_{H\rm bcc}$ in Eq. (3) given by D-D from -1.6585 to -1.586. This step is reasonable since D-D, as noted above, suggest discrepancies may have followed from the neglect of higher-order anharmonic corrections.

Considering the closeness of the predicted bcc and fcc melting parameters Γ_S and Γ_L, these adjustments in fact played only a negligible role in the present study. However, they provide some measure of satisfaction by allowing us to treat Al as fcc and Mo as bcc.

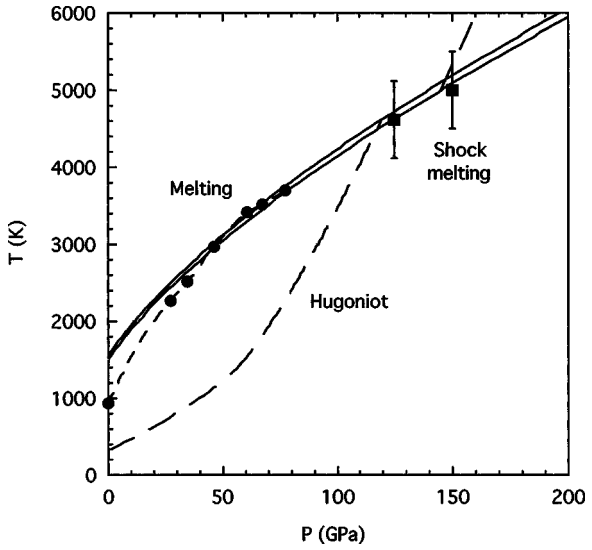

FIG. 1. Aluminum melting curve and Hugoniot. DAC measurements (Ref. 2) (filled circles). Calculated melting curves (solid curves). Calculated solid and liquid Hugoniots (dashed curves), below and above 4700 K, respectively. Shock melting points (filled boxes) at melting and freezing pressures determined from breaks in the shock sound velocity. Temperatures at the shock melting points were calculated using the Grüneisen model (Ref. 17).

III. APPLICATION TO ALUMINUM

In order to apply the inv-6 equation of state to the melting of Al two approximations were made. First, we replaced the Madelung energy in Eqs. (3)–(5) with the room-temperature isotherm determined from diamond-anvil-cell measurements and fitted to the Birch-Murgnahan (BM) equation,[16] corrected to their 0 K values. The excess free energy, total energy, and pressure for each phase may be expressed as

$$F_e = U_{\rm BM} + F_{\text{th-inv6}}, \quad (6)$$

$$E = U_{\rm BM} + 1.5NkT + U_{\text{th-inv6}}, \quad (7)$$

and

$$P = P_{\rm BM} + \frac{NkT}{V} + \frac{n}{3}\frac{U_{\text{th-inv6}}}{V}. \quad (8)$$

The second approximation involves determining the value of B in the potential (1). Vocadlo and Alfe calculated the melting curve for fcc aluminum employing density functional theory molecular dynamics and an inverse-6.7 power potential reference system with $B=247$ eV cm$^{6.7}$, which best represented their liquid simulations.[13] By using the value of $B=227$ eV cm^6 in Eq. (1) with $n=6$ we are able to calculate a melting curve and Hugoniot that are in excellent agreement with melting measurements made in a laser-heated DAC.[2]

The melting curves shown in Fig. 1 were calculated by two methods. In the first we utilized the scaling properties of the inverse-power potentials. By using Eq. (2), a set of melting temperatures and volumes could be chosen such that $\Gamma_S=95.34$ for the solid and $\Gamma_L=92.98$ for liquid freezing. The calculated pressures appear as the two parallel curves, the lower curve being the solid melting curve. In a second

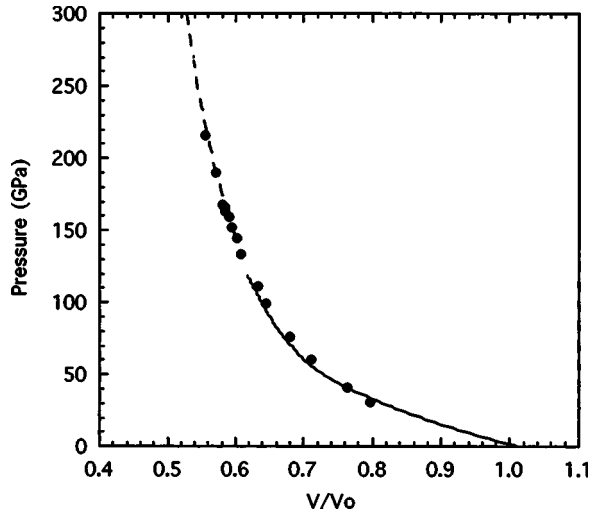

FIG. 2. Aluminum Hugoniot. Experimental data (filled circles) (Refs. 17b,17c). Hugoniot calculations for solid (solid curve) and liquid (dashed curve).

method the melting point was determined at a given temperature by calculating the difference in the solid and liquid Helmholtz free energies ΔF at a series of volumes and then determining the volume at which $\Delta F=0$. The pressure of the transition can be estimated by averaging the pressures of the two coexisting phases at the volume where $\Delta F=0$. This method is useful for those cases, such as metals, where the volume change across the transition is very small, about 1.3% in the case of Al. The melting obtained using this second method is not plotted, but lies, as expected, between the solid melting and liquid freezing curves determined using the first method.

The solid and liquid Hugoniots shown in Figs. 1 and 2 were calculated by satisfying the equation

$$E - E_0 = 0.5(P + P_0)(V_0 - V), \tag{9}$$

where the subscripted variables are initial conditions in the solid at 298 K. The melting and freezing curves, shown in Fig. 1, cross the calculated Hugoniot at 120 and 150 GPa, respectively, in good agreement with the experimentally determined values of 125 and 150 GPa. The experimental shock melting pressures were determined from breaks in the shock sound velocity, but the temperature, not measured, had been estimated using the Grüneisen model.[17(a)]

IV. MOLYBDENUM

Molybdenum, which melts from the bcc phase at 2890 K, is known to be stable in this structure at room temperature to a pressure of at least 416 GPa.[18] The stability of the bcc phase, relative to close packed, is accounted for by a gap in the electron density of states (DOS) near the Fermi energy.[19,20] The driving force for a transition to hcp at higher pressure is believed to be a pressure-induced *s-p* to *d* electron transfer.[21,22]

There is experimental and theoretical evidence which shows that upon melting changes occur in the atomic ordering of liquid Mo, and other bcc transition metals, which influence the valence electronic structure.[23–25] Since it is well known that the bcc and fcc structures of transition metals have electron density of states (DOS) which differ significantly,[21,22] then it should be expected that the melting of the eightfold coordinated bcc structure to a more closely packed liquid structure will lead to changes in the DOS. Time resolved photoelectron spectroscopy measurements for these metals show changes in the DOS in the solid and liquid which reflect the changes in atomic ordering from bcc to a close-packed-like ordering.[23–25]

Ab initio molecular dynamics simulations for open-shell transition metals also predict changes from a bcc structured DOS in the solid, with peaks and valleys, to a smoothed DOS in the liquid.[26–28] In contrast to the open-shell transition metals, the DOS of Cu, which has a filled *d* band changes only slightly upon melting.[28,29]

In effect, experiment and theory tell us that upon melting, both the atomic and the electron system in an open shell transition metal undergo a structural rearrangement. The significance of these results for melting is that, while the free energy changes resulting from atomic reordering are treated quite naturally by the statistical mechanical models, the differing contributions of the solid and liquid *d*-electron systems must also be included.

A. Friedel model

We extend our Al model to Mo by writing the excess free energy of the solid and liquid phases as the sum of contributions from the M static lattice, the inv-6 potential thermal free energy, and add the *d*-band cohesive energy

$$F_e^s = U_{\mathrm{M}} + F^s_{\text{th-inv6}} + U^s_{d\text{-band}} \tag{10}$$

and

$$F_e^l = U_{\mathrm{M}} + F^l_{\text{th-inv6}} + U^l_{d\text{-band}}. \tag{11}$$

For the *d*-band cohesive energy $U_{d\text{-band}}$ we employ the well known Friedel model[8]

$$U_{d\text{-band}} = -\frac{W}{20} n_d (10 - n_d). \tag{12}$$

W is the bandwidth and n_d is the effective number of *d* electrons per ion. Since we treat W as temperature independent the thermal properties determined by the inv-6 EOS remain unaffected.

The Friedel model has proven successful in describing the variation of the cohesive energy of transition metals and their alloys with the filling of the *d* band.[30] The cohesion is a maximum at the middle of a series (near Mo) when all five bonding states are filled and the antibonding states are empty. The contribution of the Friedel term to the pressure is then

$$P_{d\text{-band}} = \frac{\partial W}{\partial V} n_d (10 - n_d)/20. \tag{13}$$

The volume dependence of W has been described by $W = W_0 (R^0_{\mathrm{WS}}/R_{\mathrm{WS}})^n$, where W_0 and R^0_{WS} correspond to the equilibrium band width and Wigner Seitz radius. n is a pa-

rameter obtained from electron-band theory calculations. Since the function W increases with decreasing volume $P_{d\text{-band}}$ decreases with increasing compression. Values for W_0 and n_d and n have been determined across the transition series. For bcc Mo, Pettifor[31] has calculated values of $W_0=9.5$ eV and $n=4.3$. We assume that the liquid phase can also be treated using the Friedel model, but with slightly different electronic properties.

Since the DAC solid isotherm, as represented by the BM fit, already includes the U_M and $U_{d\text{-band}}$ terms we avoid double counting and rewrite Eqs. (10) and (11) as

$$F_e^s = U_{\mathrm{BM}} + F_{\text{th-inv6}}^s, \tag{14}$$

and

$$F_e^l = U_{\mathrm{BM}} + F_{\text{th-inv6}}^l + \delta U_{d\text{-band}}^{l-s}, \tag{15}$$

where $\delta U_{d\text{-band}}^{l-s}=(U_{d\text{-band}}^l - U_{d\text{-band}}^s)$ is the change in d-band cohesive energy going from the solid to liquid phase. The $\delta U_{d\text{-band}}^{l-s}$ term, which is small, is essential in the case of melting.

B. Melting

Since there is little in the way of data for W_o and n_d available for liquid transition metals we assume that the liquid is effectively a close-packed fcc-like system. We rely on Moriarty's[21] calculation for estimates of n_d for bcc and fcc Mo calculated over a twofold range in density. Moriarty found that n_d increased from about 4.2 electrons at normal density to about 4.72 at twofold compression and that fcc had an n_d higher by about 0.1 electrons. To the extent that the liquid coordination number may be fcc-like we assume that the fcc values approximate those of the liquid. Since the parameter n increases with increasing n_d, then n must increase upon melting. A trial value of $n=4.4$, increased from 4.3 in the solid, was set for the liquid. A value for B, of 400 eV cm^6, was obtained for the inverse-6 potential (1) by requiring that the normal melting point for Mo approximate the experimental value of 2890 K.

Melting points were obtained at a given temperature by calculating the difference in the liquid and solid Helmholtz free energies,

$$\Delta F = (F_{\text{th-inv6}}^l - F_{\text{th-inv6}}^s) + \delta U_{d\text{-band}}^{l-s} \tag{16}$$

at a series of volumes and then determining the volume at which $\Delta F=0$. The first term in parentheses, represents the change in the ion free energy and the second term is the contribution due to the change in d-band cohesive energy. Figure 3 shows the DAC measurements, the melting curves calculated by including, and omitting, the $\delta U_{d\text{-band}}^{l-s}$ term. Also shown are calculated solid and liquid Hugoniots.

The melting curve calculated by including the $\delta U_{d\text{-band}}^{l-s}$ term in Eq. (16) is in good agreement with the DAC measurements which show a slow rise in the temperatures up to 40 GPa with a flattening of the melting slope to $dT/dP\sim 0$ above that pressure. But above 90 GPa the model predicts that the temperatures begin to decrease and cross the solid Hugoniot near 181 GPa and 2639 K. The predicted decrease

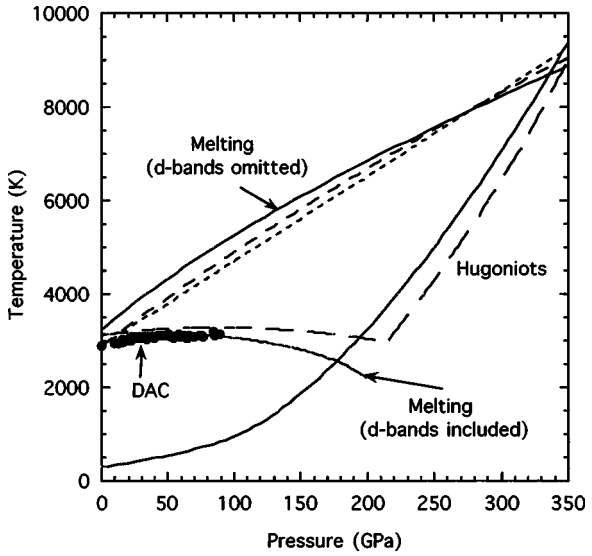

FIG. 3. Molybdenum melting curve and Hugoniot. DAC melting measurements (Ref. 3) (filled circles). Melting curves calculated with and without d bands as denoted (solid curves). Melting curve with modified liquid d-band parameter described in text (large dashed curve). Melting calculations of Moriarty (Ref. 21) (dotted curve) and Burakovsky (Ref. 32) (small dashed curve). Calculated Hugoniots: solid (solid curve) and liquid (dashed curves).

is possibly due to our limited knowledge of the Friedel model parameters at high density and sufficient information, now lacking, for properly modeling the free energy of liquid transition metals. By lowering the value of n slightly, from 4.4 to 4.39, the melting temperature near 220 GPa could be raised from 2205 to 3011 K. On the matter of why changing n from 4.4 to 4.39, has such a large effect, consider that the values of n originally used are $n=4.3$ for the solid and 4.4 for the liquid, a difference of 0.10. Then, a decrease in the liquid n, from 4.4 to 4.39, is in fact overall a −10% change. The original prediction of a negative slope may in fact be correct since the appearance of negative melting slopes in d-electron systems is well known and is reviewed here in Sec. VI.

By omitting the $\delta U_{d\text{-band}}^{l-s}$ term, the predicted melting curves are in agreement with the steep curves calculated by Moriarty,[21] using pair potentials, and by Burakovsky *et al.*[32] using a dislocation model with Lindemann-like scaling. These melting curves are all aluminumlike. For example, shock melting was observed in Al near 125 GPa and 4700 K (Fig. 1) that matches well to the "d bands omitted" curves in Fig. 3.

The importance of including the partially filled d-band free energy is demonstrated numerically in Fig. 4 where the calculated values are plotted for $(F_{\text{th-inv6}}^l - F_{\text{th-inv6}}^s)$ and $\delta U_{d\text{-band}}^{l-s}$ at a series of temperatures at 75 GPa. Melting occurs at $\Delta F=0$. The contribution of $\delta U_{d\text{-band}}^l$ at this pressure is 0.128 eV/atom, which is about 1% of W. This reduction in the liquid free energy, even while numerically small, leads to a decrease in the melting temperature from 4942 K (on the d bands omitted curve in Fig. 3) to 3170 K (on the DAC experimental curve). The associated pressure drop due to the $\delta U_{d\text{-band}}^{l-s}$ term is small, −5 GPa, but not negligible.

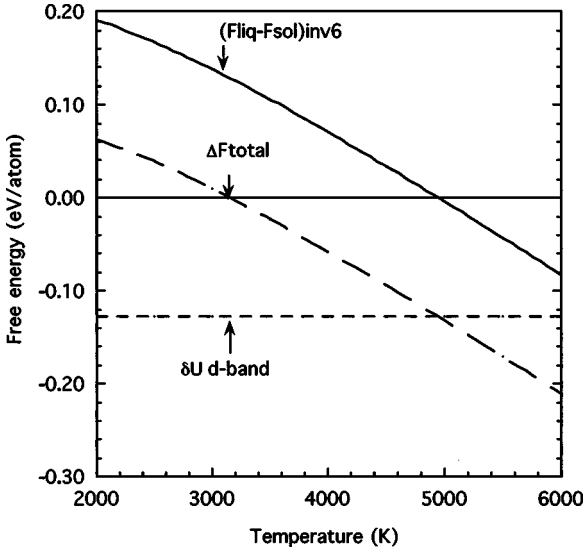

FIG. 4. Contributions to the excess free energy at a series of temperatures near 75 GPa. ($F^{l}_{\text{th-inv6}} - F^{s}_{\text{th-inv6}}$) is the change in the ion free energy (solid curve). $\delta U^{l-s}_{d\text{-band}}$ is the change in *d*-band cohesive energy (small dashed curve). Melting occurs at $\Delta F_{\text{total}} = 0$ along the dash-dotted curve.

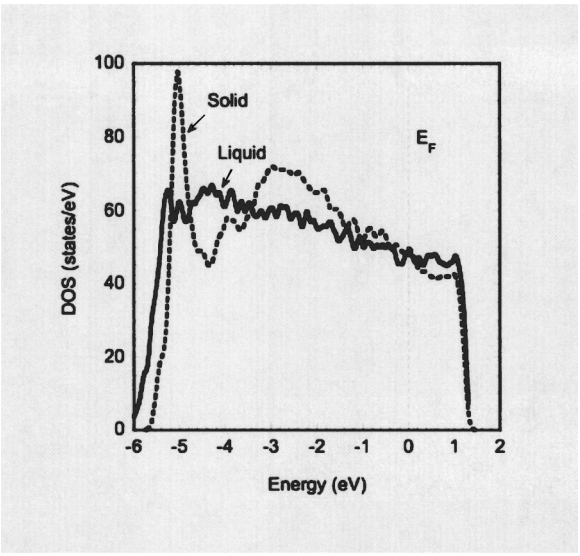

FIG. 5. Calculated DOS for liquid (solid curve) and solid Mo (dashed curve) made at temperatures of 4956 and 3459 K, respectively. The Fermi energy (E_F) is at energy = 0.

C. Electron density of states (DOS)

While the use of quantum molecular dynamics (QMD) simulations to carry out the accurate free energy calculations needed for the melting of transition metals remains a future goal, the method can now be useful for evaluating the quality of specific modeling approximations. QMD calculations were performed for 54-atom Mo systems in the solid (at 3459 K) and liquid (at 4960 K) states in a periodic box, respectively. A plane-wave pseudopotential method was used for the electronic structure calculation while the ionic trajectories were proceeded by the classical equation of motion. At each time step, the ionic positions were determined using the Hellman-Feynman forces obtained from electronic structures calculation in which the Bohn-Oppenheimer approximation is applied. The initial configurations for the 54-atom solid and liquid states were generated based on interatomic potentials derived from the modeled generated pseudopotential theory (MGPT).[21,26] The systems were equilibrated for 15 picoseconds using MGPT potentials and then passed on to the first-principles MD calculations where the systems were further equilibrated for 0.5 ps and then ran for 3–4 picoseconds to gather statistics.

Figure 5 shows the calculated electron density of states (DOS) for liquid and solid Mo made at temperatures of 4956 and 3459 K, respectively. While the plots may have only a semiquantitative significance they do indicate that the DOS in the liquid is smoother and broader than in the solid, leading to a larger value of *W* larger by about 0.3 eV/atom. These results are consistent with those of Moriarty that showed the melting of the solid led to about a 0.3 eV/atom lowering of the Fermi energy.[26]

D. Comparison with transitions reported in shock experiments

Returning to Fig. 3, an extrapolation of the experimental melting measurements shows that it crosses the Hugoniot near 210 GPa and 3200 K. This is in excellent agreement with the pressure at which the break in the shock sound velocity was observed by Hixson *et al.*,[33] that had been attributed to a bcc-fcc transition. In addition to the transition at 210 GPa, Hixson *et al.*[33] observed a second break in the shock sound velocity near 390 GPa, at a calculated temperature near 10 000 K, which they attributed to melting of the bcc solid.

At 210 GPa and 3200 K, the pressure and temperature at which the Friedel model solid melting curve crosses the Hugoniot has the value of $\Gamma \sim 200$. This high value is a consequence of the large depression in the melting temperature caused by the *d* electrons and suggests that the melt is highly viscous. If the second break in the experimental shock data is real, we speculate that it may represent the transition from the viscous fluid to a normal liquid, but at a temperature much below 9000 K.

Some evidence for the presence of a highly viscous state in transition metal melts has been reported by Brazhkin and Lypkin.[34] The authors carried out quenching experiments on transition metal melts for which an inspection of the grain size suggested strongly that the melts are very viscous and that the viscosity grows considerably along the melting curve. Brazhkin and Lypkin note that this appears to be the case in Fe, providing some basis to the theory that the liquid in the Earth's core is highly viscous.

V. MELTING OF THE ACTINIDE METALS

The chemical bonding in transition metals, and light actinides Th to Pu, are known to have strong similarities in that transition metal bonding is due to delocalized *d* electrons and light actinide bonding by delocalized *f* electrons. Bonding in the heavy actinides (Am and beyond) are characterized by more localized *f* orbitals. Pu is located at the border of the light and heavy actinides. The unusual room temperature low

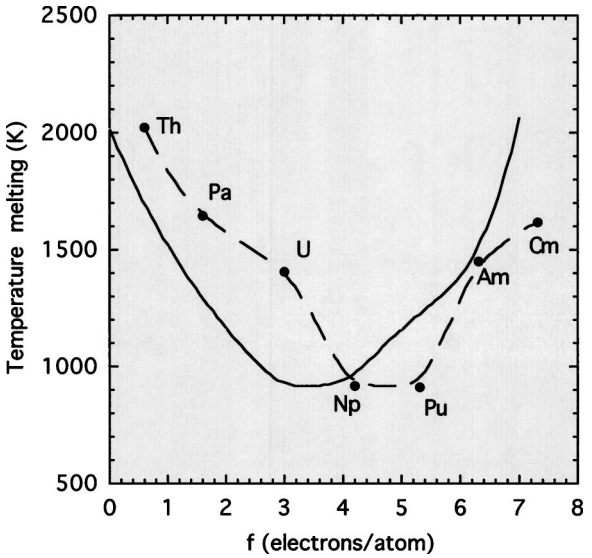

FIG. 6. Calculated ambient melting temperatures of the "hypothetical light actinides series" (solid curve). The f-electron occupancy for each of the elements was taken from the theoretical values reported by Söderlind *et al.* (Ref. 42).

coordinated structures of the light actinides are believed due to the f-electron character.[35]

Two related properties of the light actinides are particularly noteworthy. The equilibrium room temperature volumes decrease from Th to a mininum at Pu then rise to Am and Cm.[36] The ambient melting temperatures of the light actinides are anomalously low and decrease starting from Th, also reaching a minimum near Np and Pu, then rise for the heavier actinides.[37] See Fig. 6. Using a model, similar to ours and included the Friedel expression to calculate the f-band energy, Johansson and Skriver,[38] explained the trend in the volume as being directly related to the increase in f-electron bonding. To explain the anomalously low melting points Kmetko and Hill[39] suggested that the angular dependence of f-electron wave functions favored bonding in the liquid rather than the bcc phase. In a general sense, this is consistent with the view of transition metal melting that we have developed in this report.

Rather than calculate the ambient melting temperatures specifically for each of the light actinides, we constructed a "hypothetical light actinide" series by simply adding f electrons to thorium which, as with all of the light actinides, melts from the bcc structure. Th is often considered as a transition metal with small f character and a rather broad band of unoccupied $5f$ states above the Fermi level. By increasing the f electron occupancy systematically we are able to simulate roughly the change in melting temperature across the light actinide series.

The theoretical model is the same as used in Sec. IV, except the Friedel term is written for f bands,

$$U_{f\text{-band}} = -\frac{W_f}{28} n_f (14 - n_f), \tag{17}$$

with the remaining expressions for the pressure and free energy unchanged. For W_f, the f-band width, we use the simple formula and parameters employed by Johannson and Skriver,[39] $W_f = W_f^0 (V_0/V)^2$, where W_0 and V_0 correspond to the equilibrium band width and volume, respectively. n_f is f-electron occupation number. $W_0 = 3.6$ eV.

The Birch-Murgnahan fit to the lattice pressure and energy came from the work of Bellussi *et al.*[40] We retained the use of the inverse sixth power potential with a value for $B = 1050$ eV cm^6 and fit the melting point of thorium approximately by using an n_f occupation number of 0.4. Wills and Eriksson[41] calculated that for Pa and U the fcc lattice has an f-electron occupancy about 1.5 to 5% higher than for bcc. In the melting calculations described we chose an intermediate value, that the n_f in a close-packed liquid was higher by 1.025 (or 2.5%) than in the bcc solid.

Melting points were determined, as in earlier sections, by calculating the difference in the solid and liquid Helmholtz free energies, at a series of volumes, at a given temperature and then determining the volume at which $\Delta F = 0$. Figure 6 shows the ambient melting temperatures plotted as a function of f-electron occupancy. The f-electron occupancy for each of the elements was taken from the theoretical values reported by Söderlind *et al.*[42] Calculations were made at integral values.

The predicted melting temperatures of our "hypothetical light actinide" are in good qualitative agreement with experiment. The model predicts a decrease in the melting temperature with increasing f electrons, with a minimum near 3–4f electrons compared to the experimental 4–5f electrons. The divergence of the two curves above 6 f electrons is likely a consequence of an increasing level of localized bonding.

VI. DISCUSSION

The association of low melting slopes with d-electron character is widespread and not limited to transition metals. It is well known that in the case of the alkali and alkaline-earth metals the pressure induced increase of the d-electron occupation number causes a flattening of the potassium melting curve above 4 GPa and the appearance of complex structures in Ba, Sr, and Ca.[43] In the case of Rb and Cs, negative melting slopes ($dT/dP < 0$) lead to a temperature minima and maxima below 10 GPa.[44] In effect, pressure transforms the heavy alkali and alkaline metals to early transition metals. The low melting slopes of the bcc transition metals, with high binding energies, represent the limiting cases of this trend.

The influence of d electrons on melting at high pressure is nicely provided by a comparison of Al (Ref. 2) and Mo (Ref. 3) with Mg.[43] At room temperature, Mg transforms from hcp to bcc at 50 GPa (Ref. 45) while Al remains fcc up to 220 GPa, the highest pressure for which measurements were made.[16] The melting curves of all three metals were measured at Mainz using the same experimental setup. The melting curve of Mg which, similar to Al, is a nearly free electron polyvalent metal, follows that of Al up to the hcp-bcc transition pressure of 50 GPa. Above 50 GPa the melting slope of Mg decreases and bends parallel to the melting curve of Mo while the Al melting curve continues to rise. Theoretical calculations have shown that the increase in d character is

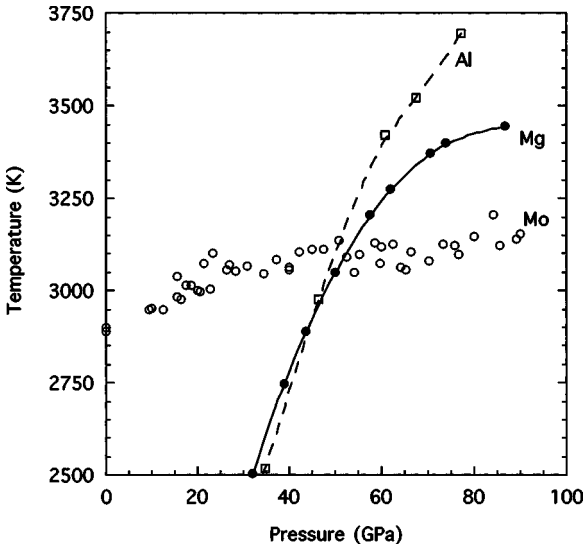

FIG. 7. Melting curves of Al (Ref. 2), Mg (Ref. 43), and Mo (Ref. 3). Near 50 GPa Mg transforms from hcp to bcc (Refs. 45,46).

responsible for the transition.[46] This suggests that the melting slope of Al will also show a decrease upon approaching its fcc-bcc transition pressure (see Fig. 7).

It is well known that an accurate prediction of the bcc-hcp transition in a metal requires a detailed calculation of the electron density of states of both structures.[19,20] Clearly then, an accurate prediction of the bcc-liquid transition must also require a detailed calculation of the electron density of states of both phases. These difficulties may be compounded by the directional bonding of *d* and *f* electrons which introduce the likelihood of localized ordering.[39,47,48] Consequently, one cannot employ an effective interatomic potential determined from a fit to solid state properties and expect to obtain a reliable melting curve for an open valence shell metal. While such an approximation may be adequate for calculating equations of state, phase diagrams are much more sensitive to relatively small details in the free energy. In this regard open shell metals differ profoundly from those of rare gases and nearly free electron metals, such as Ar, Al, and even Cu, where the electronic structure, hence the effective interatomic forces, remain relatively unchanged upon melting.

Since a rigorous prediction of melting temperature requires a phase matching of free energy and pressure at constant temperature, improvements in the melting theory of metals need first be directed toward obtaining a more detailed understanding of the density dependent electronic properties of the liquid employing a systematic approach similar to that which has been done for the solid.[19,20,31]

ACKNOWLEDGMENTS

We thank Dr. Daniel Errandonea and Dr. Per Söderlind for helpful comments. Work by M.R. and L.H.Y. was performed by the University of California under the auspices of the U.S. DOE by the Lawrence Livermore National Laboratory. M.R. also wishes to thank the Max-Planck-Institute für Chemie at Mainz for its continued hospitality.

[1] R. Boehler, Nature (London) **363**, 534 (1993).
[2] R. Boehler and M. Ross, Earth Planet. Sci. Lett. **153**, 227 (1997).
[3] D. Errandonea, B. Schwager, R. Ditz, R. Boehler, and M. Ross, Phys. Rev. B **63**, 132104 (2001).
[4] D. Errandonea, M. Somayazulu, D. Häusermann, and D. Mao, J. Phys.: Condens. Matter **15**, 7635 (2003).
[5] D. Alfe, L. Vocadlo, G. D. Price, and M. J. Gillan, J. Phys.: Condens. Matter **16**, S973 (2004).
[6] F. Ducastelle, J. Phys. (France) **31**, 1055 (1970).
[7] D. G. Pettifor, *Bonding and Structure of Molecules and Solids* (Clarendon Press, Oxford, 1995).
[8] J. Friedel, in *The Physics of Metals I*, edited by J. Ziman (Cambridge University Press, Cambridge, 1969), p. 340. Also see, J. A. Alonso and N. H. March, *Electrons in Metals* (Academic Press, London, 1989).
[9] (a) W. G. Hoover, M. Ross, K. W. Johnson, D. Henderson, J. A. Barker, and B. C. Brown, J. Chem. Phys. **52**, 4931 (1970); (b) W. G. Hoover, S. G. Gray, and K. W. Johnson, *ibid.* **55**, 1128 (1971).
[10] H. E. DeWitt, *Strongly Coupled Plasmas (1978)*, edited by G. Kalman and P. Carini (Plenum, New York, 1979), p. 81.
[11] B. B. Laird and A. D. J. Haymet, Mol. Phys. **75**, 71 (1992).
[12] D. H. E. Dubin and H. DeWitt, Phys. Rev. B **49**, 3043 (1994).
[13] L. Vocadlo and D. Alfè, Phys. Rev. B **65**, 214105 (2002).
[14] D. Alfè, G. Kresse, and M. J. Gillan, Phys. Rev. B **61**, 132 (2000).
[15] W. G. Hoover, D. A. Young, and R. Grover, J. Chem. Phys. **56**, 2207 (1972).
[16] R. G. Greene, H. Luo, and A. L. Ruoff, Phys. Rev. Lett. **73**, 2075 (1994).
[17] (a) J. W. Shaner *et al.*, in *High Pressure Science and Technology*, edited by C. Homan, R. K. MacCrone, and E. Whalley (North Holland, Amsterdam, 1984), pp. 137–141; (b) L. V. Altshuler *et al.*, Sov. Phys. JETP **11**, 573 (1960); (c) A. C. Mitchell and W. J. Nellis, J. Appl. Phys. **52**, 3363 (1981).
[18] A. L. Ruoff, H. Xia, H. Luo, and Y. K. Vohra, Rev. Sci. Instrum. **61**, 3830 (1990).
[19] H. L. Skriver, Phys. Rev. B **31**, 1909 (1985).
[20] D. G. Pettifor, J. Phys. C **3**, 367 (1970).
[21] J. A. Moriarty, Phys. Rev. B **45**, 2004 (1992).
[22] J. A. Moriarty, Phys. Rev. B **57**, 10 340 (1998).
[23] P. Oelhafen, R. Wahrenberg, and H. Stupp, J. Phys.: Condens. Matter **12**, A9 (2000).
[24] H. Stupp, H.-G. Boyen, G. Gantner, and P. Oelhafen, J. Non-Cryst. Solids **170**, 1 (2000).
[25] R. Wahrenberg, H. Stupp, H.-G. Boyen, and P. Oelhafen, Europhys. Lett. **49**, 782 (2000).
[26] J. A. Moriarty, Phys. Rev. B **49**, 12 431 (1994).
[27] W. Jank, Ch. Hausleitner, and J. Hafner, J. Phys.: Condens. Matter **3**, 4477 (1991).

[28] G. Kresse and J. Hafner, Phys. Rev. B **48**, 13 115 (1993).
[29] A. Pasquarello, K. Laasonen, R. Car, C. Lee, and D. Vanderbilt, Phys. Rev. Lett. **69**, 1982 (1992).
[30] R. E. Watson and M. Weinert, Solid State Phys. **56**, 1 (2001).
[31] D. G. Pettifor, J. Phys. F: Met. Phys. **7**, 613 (1977).
[32] L. Burakovsky, D. L. Preston, and R. R. Silbar, J. Appl. Phys. **88**, 6294 (2002).
[33] R. A. Hixson, D. A. Boness, J. W. Shaner, and J. A. Moriarty, Phys. Rev. Lett. **62**, 637 (1989).
[34] V. V. Brazhkin and A. G. Lyapin, Phys. Usp. **43**, 493 (2002).
[35] P. Söderlind, J. M. Wills, and O. Erikkson, Phys. Rev. B **57**, 1320 (1998); P. Söderlind, Adv. Phys. **47**, 959 (1998).
[36] W. H. Zachariasen, J. Inorg. Nucl. Chem. **35**, 3487 (1973).
[37] J. L. Smith and E. A. Kmetko, J. Less-Common Met. **90**, 83 (1989).
[38] B. Johansson and H. L. Skriver, J. Magn. Magn. Mater. **29**,217 (1982).
[39] E. A. Kmetko and H. H. Hill, J. Phys. F: Met. Phys. **6**, 1025 (1976).
[40] G. Bellussi, U. Benedict, and W. B. Holzapfel, J. Less-Common Met. **78**,147 (1981).
[41] J. M. Wills and O. Eriksson, Phys. Rev. B **45**, 13 879 (1992).
[42] P. Söderlind, B. Johansson, and O. Eriksson, Phys. Rev. B **52**, 1631 (1995).
[43] D. Errandonea, R. Boehler, and M. Ross, Phys. Rev. B **65**, 012108 (2001).
[44] R. Boehler and C.-S. Zha, Physica B **139&140**, 233 (1986).
[45] H. Olijnyk and W. B. Holzapfel, Phys. Lett. **100**, 191 (1984).
[46] A. K. McMahan and J. A. Moriarty, Phys. Rev. B **27**, 3235 (1983).
[47] G. W. Lee, A. K. Gangopadhyay, K. F. Kelton, R. W. Hyers, T. J. Rathz, J. R. Rogers, and D. S. Robinson, Phys. Rev. Lett. **93**, 037802 (2004).
[48] P. Söderlind, O. Eriksson, B. Johansson, J. W. Wills, and A. M. Boring, Nature (London) **374**,524 (1995).